RESEARCH PAPER

PCCP
www.rsc.org/pccp

A novel long path photolysis cell—application to the reactivity of selected organic compounds toward the nitrate radical (NO_3)

Davy Rousse and Christian George*

Laboratoire d'Application de la Chimie à l'Environnement (UCBL-CNRS) 43 boulevard du 11 Novembre 1918, F-69622, Villeurbanne, France. E-mail: christian.george@univ-lyon1.fr; Fax: +33 (0)4 72 44 8114; Tel: +33 (0)4 72 43 1489

Received 7th January 2004, Accepted 2nd March 2004
First published as an Advance Article on the web 14th April 2004

Bimolecular rate coefficients for the reactions of the nitrate radical, NO_3, with methanol, ethanol, acetaldehyde *tert*-butyl methyl ether, propionic acid, dimethylmalonate, dimethylsuccinate, dimethyl carbonate and diethylcarbonate in aqueous solutions have been measured using a novel experimental approach. This study was performed using laser flash photolysis (LFP) with a capillary made of Teflon AF2400 as a long path capillary photolysis cell. Taking benefit of this new material allowing a long optical path length for a very limited irradiated solution volume, new rate constants were established. All experiments were carried out at room temperature. Measured rate coefficients for the reaction of the NO_3 radical with methanol, ethanol, acetaldehyde, dimethylcarbonate, diethylcarbonate, dimethylmalonate, dimethyl succinate, propionic acid and *tert*-butyl-methyl ether are (units are 10^5 M^{-1} s^{-1}): $k_{NO_3+\text{ethanol}} = 4.8 \pm 0.5$, $k_{NO_3+\text{ethanol}} = 19 \pm 3$, $k_{NO_3+\text{acetaldehyde}} = 20 \pm 3$, $k_{NO_3+\text{dimethylcarbonate}} = 0.15 \pm 0.04$, $k_{NO_3+\text{diethylcarbonate}} = 0.84 \pm 0.12$, $k_{NO_3+\text{dimethylmalonate}} = 0.26 \pm 0.07$, $k_{NO_3+\text{dimethylsuccinate}} = 0.34 \pm 0.02$, $k_{NO_3+\text{propionic acid}} = 0.77 \pm 0.02$, $k_{NO_3+\textit{tert}\text{-butyl-methyl ether}} = 3.9 \pm 1.3$. The uncertainties in the above expressions are $\pm 2\sigma$ and represent precision only. The reported rate coefficients for the reactions of NO_3 with methanol, ethanol and acetaldehyde agree well with currently recommended values. To date, there is no kinetic data reported in the literature for the NO_3 radical reaction with dimethylcarbonate, diethylcarbonate, dimethylmalonate, dimethylsuccinate, propionic acid and *tert*-butyl-methyl ether. The reaction mechanism is briefly discussed as a function of bond energies

Introduction

The atmosphere can be considered as a giant chemical reactor where gases and aerosols play a key role in all chemical and physical processes linked to the Earth's climate. The presence of condensed matter renders this reactor quite inhomogeneous with complex exchanges between all phases encountered in the atmosphere.[1]

In the atmospheric gas phase, the nitrate radical (NO_3) has been identified as a key oxidant, especially at night when the importance of the hydroxyl radical (OH) is decreasing. Accordingly, numerous studies focused on the kinetics and on the addition and hydrogen-abstraction mechanisms in which NO_3 is involved.[2,3]

However, since the Earth's atmosphere is far from being purely gaseous as it contains also aqueous particles, *i.e.* the so-called hydrometeors (clouds and fogs). As the nitrate radical may undergo phase partitioning[4] or has direct sources in the aqueous phase, many of its reactions are also occurring in water.[2] Therefore, the nitrate radical is a key oxidant also in the aqueous phase, along with the hydroxyl radical (OH).

In our previous paper,[5] we discussed the reactivity of the hydroxyl radical toward some oxygenates, and new rate coefficients were established for the OH + dimethylmalonate, OH + dimethylsuccinate, OH + dimethylcarbonate and OH + diethylcarbonate reactions, followed by a discussion on the H-abstraction mechanism. In the present study however, we focused on the reactivity of NO_3 toward a few oxygenates.

Although many studies have dealt with the kinetics of the reaction between NO_3 and a series of organic compounds, very few studies have been performed for the reactions of NO_3 with the intermediate-sized aliphatic compounds (*i.e.* C_2–C_{10}), and especially for the reactions of OH with organics containing oxygenated polyfunctional groups.

Such interest stems from the fact that the intermediate length carbon chain and oxygenated hydrocarbon compounds are expected to be increasingly used as new industrial solvents to favour water based technology. Currently, C_2–C_{10} dibasic esters[6–8] and carbonates[9,10] are being considered to replace "old" additives to obtain "new" environmentally friendly solvents. However, the atmospheric degradation of dibasic esters and carbonates will potentially result in the formation of tropospheric ozone and other secondary pollutants.[7] Moreover, the C_2–C_{10} oxygenated organics can potentially form low vapour pressure secondary reaction compounds that can be either taken up by clouds or form secondary aerosols[11,12] (SOA). In turn, these compounds can be removed from the atmosphere *via* rainfall, dry or wet deposition and potentially act as a source of organic pollutants in surface waters.

To date, the atmospheric fate of C_2–C_{10} dibasic esters and carbonates remains uncertain. In the atmosphere, these compounds are likely to be involved in multiphase chemistry and be removed *via* the attack by OH or NO_3.

In this paper, we present new determinations of the kinetics of the hydrogen abstraction reactions between NO_3 and some oxygenates, *i.e.* methanol, ethanol, acetaldehyde *tert*-butyl methyl ether, propionic acid, dimethylmalonate, dimethylsuccinate, dimethyl carbonate and diethylcarbonate. This study has been performed using laser flash photolysis (LFP) in a capillary made of Teflon AF2400 as a long path capillary photolysis cell. Taking benefit of this new material allowing a long optical path length for a very limited irradiated solution volume, new rate constants were established.

DOI: 10.1039/b400175c

Details of the experimental procedure that were employed to study these reactions in aqueous solutions are given below.

Experimental

Laser photolysis apparatus

The NO_3 radical was produced by the laser-flash photolysis of peroxodisulfate or cerium ammonium nitrate precursors.[2] The experimental setup described in this section has been applied for photolytic generation of sulfate radical from peroxodisulfate. Sulfate radicals were then converted into nitrate radical in the presence of excess nitrate anion:

$$S_2O_8^{2-} + h\nu \rightarrow 2SO_4^{\bullet -} \quad (R1)$$

$$SO_4^{\bullet -} + NO_3^- \rightarrow SO_4^{2-} + NO_3^{\bullet} \quad (R2)$$

Using reactions (R1) and (R2) implies a certain time to achieve complete formation of the nitrate radical. This time the gap depends on laser fluence and concentration of reactants. Therefore, depending on experimental conditions, the decay of the nitrate radical may not necessarily be of first order during the first microseconds following the laser discharge (as shown in Fig. 2). Therefore, care must be taken when analysing NO_3 decays to be in a time region where the production of NO_3 is complete.

Nitrate radicals were also produced from the photolytic reaction on cerium nitrate ammonium complex, as an alternative to the experimental method mentioned above. Solutions of Ce(IV) complex in nitric acid were used to generate nitrate radical.

$$[Ce^{IV}(NO_3)_6]^{2-} + H_2O + h\nu \rightarrow [Ce^{III}(NO_3)_5H_2O]^{2-} + NO_3^{\bullet} \quad (R3)$$

Typical Ce(IV) complex concentration was in the range 5×10^{-4}–5×10^{-3} mol L^{-1}. Typical experimental nitric acid concentration was 1.0 mol L^{-1}.

A Lambda Physik Excimer Multigas laser (EMG 101), operated with a Xe/F_2 mixture leading to a lasing wavelength at 351 nm was used as the photolysis source. Under optimum conditions, this laser produces a pulse half-width of 16 ns and a beam cross-sectional area of 250 mm^2 with an output of 125 mJ per pulse. This energy was periodically checked using a calibrated Joule-meter (Labmaster E, Coherent Inc.).

Transient species produced by the pulsed laser beam were monitored by means of time resolved absorption spectroscopy. A diode laser, with an output wavelength of 635 nm and a power of 1 mW was used as the analyzing light. The light escaping the photolysis cell (described below) was fed onto the active surface of an amplified photodiode. The rise time (5 to 95%) of the amplified photodiode was always kept below 0.5 ns.

The continuous optical signal was first measured before the laser discharge by a sample-and-hold circuit and the corresponding voltage was read by a multimeter (Keithley 179A). The transient optical absorption signal produced by the laser beam was subsequently collected by a Tektronix oscilloscope (type 2430A) *via* a differentiating circuit, which allows the change of absorption to be measured with a high sensitivity. This oscilloscope allows a maximum sampling rate of 100 MHz and has signal-averaging capacities. The full absorption may then be reconstructed from both continuous and transient signals once both of them have been transferred to a computer *via* IEEE-488 GPIB interface from the oscilloscope and multimeter. All devices were synchronized *via* a delay generator (DG535, Stanford Research System) which was operated as the master in our optical chain.

The signal to noise ratio of the measured kinetic curves was such that in most cases experiments were performed on a single shot basis. However when necessary (*i.e.*, for low NO_3 concentrations), the averaging capacities of the oscilloscope were used. In that case, up to 16 single shot experiments were averaged before transmitting to the computer. In all cases, the photolysis cell content was fully renewed between each laser pulse. We ensured that single and averaged signals led to the same kinetic determination.

Teflon AF photolysis cell

The centrepiece of the experimental set-up is a liquid core waveguide (LCW) made of Teflon AF 2400 (BioGeneral, San Diego, CA). Tubing made from these polymers have been shown to exhibit excellent optical properties such as high optical clarity (at $\lambda \leq 200$ nm more than 80% of light is transmitted through a 220 μm thick film of the polymer described above) and very low refractive index (*i.e.*, $n = 1.29$ for Teflon AF 2400 grades). The refractive index observed for the Teflon AF 2400 tube is lower than virtually all standard temperature and pressure liquids. As a result, tubing made from the Teflon AF 2400 polymer and filled with water will conduct light.

The Teflon AF 2400 guide had an inner and outer diameter of 200 and 800 μm, respectively. The length of the LCW was varied in the course of the study from 30 to 90 cm. In all cases, the internal volume of the liquid core waveguide was less than 0.1 ml for a maximum optical path length of 90 cm. Very small liquid volumes used in the LCW (liquid core waveguide) is one of the major advantages of using waveguides compared to a standard White cell design for studying radical liquid phase reactions. A good White cell can achieve a maximum path length of a few meters (which often requires expensive lasers) in a volume of about 50–100 ml. Such a large reaction volume requires much larger flow rates to replenish the cell between laser flashes. Under the typical experimental conditions employed, the LCW can achieve much longer optical path lengths in much smaller volumes without requiring as powerful light sources as those required in standard White cell systems.

The Teflon photolysis cell used is shown in Fig. 1. The highly flexible Teflon AF 2400 tubing was loosely coiled (less than 3 cm diameter) and placed in the excimer laser beam path. The NO_3 radicals were generated within the LCW following the laser flash on the precursors, as discussed above. Since

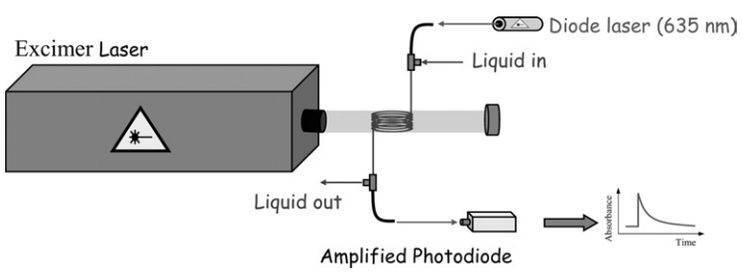

Fig. 1 Schematics of the LCW (liquid core waveguide) micro-flow tube experimental setup.

the waveguide was used as a coil, no concentration gradient could built up along the waveguide length. However, non-uniform nitrate radical concentration could be produced if the laser fluence experienced by the coild was not uniform. Therefore, in order to avoid any shielding of the front and back sides of the waveguide, the later was placed in a reactor (not shown in Fig. 1) the inner walls of which were covered by an aluminium foil. The reactor had the following dimensions $1 \times 3 \times 3$ cm^3 (height $\times$ width $\times$ depth). In this way we ensured an increased uniformity in the irradiation of the waveguide. However, we could not measure this uniformity, we therefore made sure that all kinetics studied in the present study were unimolecular (after completion of the NO_3 production as stated before).

In order to probe the solution contents of the Teflon photolysis cell, the output of the diode laser was focused on the entry of an unpolished 100-μm diameter fused silica optical fibre. The fused silica optical fibre was held in the liquid content of the photolysis cell. Then, the light was allowed to escape the solid optical fibre and was collected in the liquid core waveguide. Again, the Teflon AF tubing conducted the light up to its end where another fused silica optical (located in the liquid) collected most of this transmitted light. This second solid optical then conducted the light to the active surface of the amplified photodiode. In that way the measured signal is integrated (or averaged) over the full length of the waveguide. As the observed decays were first order, this averaging allows the determination of rate constants even in the unlikely situation where the NO_3 concentration was not uniform along the waveguide length.

The use of a long optical path-length, enabled us to work with low NO_3 concentrations. Accordingly, the UV irradiation of the nitrate precursor never led to a saturation of the latter as the nitrate radical formed was much less than 1% of the precursor concentration. The decay of the nitrate radical was monitored at a wavelength of 635 nm and was believed to obey Beer–Lambert's law.

Determination of rate coefficients

As this will be discussed in more detail in the results section, many experimental conditions have been changed (laser voltage discharge, solution composition, temperature) leading to a total of 200 experiments. In all cases reported here, the decays were purely first order decays and therefore straightforward to handle.

All kinetics were studied at room temperature, *i.e.* 298 K.

Reagents

Solutions were prepared from the following chemicals (used without further purification): $Na_2S_2O_8$ (Prolabo Normapur, 98%), $NaNO_3$ (Aldrich 100%), cerium nitrate ammonium (Aldrich $>98.5\%$), nitric acid (Aldrich 1 mol L^{-1}), perchloric acid (Aldrich 70%) methanol (Prolabo, Normapur, $>99.8\%$), ethanol (Prolabo, Normapur, $>99.8\%$), acetaldehyde (Aldrich 99.5%), dimethyl malonate (Aldrich $>99\%$), dimethyl succinate (Aldrich $>99\%$), dimethyl carbonate (Fluka $>99\%$), diethyl carbonate (Fluka $>99\%$) and *tert*-butyl-methyl ether (Aldrich $>99.8\%$). Water was taken from an 18 MΩ purification system (Millipore). In some test experiments, we used oxygen free solutions, which led to the same results as non-degassed water.

Results

Validation of the technique

In order to check the consistency of the results obtained by this technique, several well-established rate coefficients have been re-measured.

NO_3 + methanol

The kinetics of the reaction of OH with methanol (R4) has been studied before (see, for example, Table 1).

$$NO_3 + CH_3OH \rightarrow HNO_3 + CH_2OH \qquad (R4)$$

The agreement among the reported values for the rate coefficient for the reaction of OH with methanol is not very clear as values are covering more or less an order of magnitude (see Table 1) As a result, further investigations are warranted to better define the rate coefficient for the removal of OH by methanol.

A typical decay for the absorption profiles of the nitrate radical is shown in Fig. 2, whereas a typical second order plot for this reaction is shown in Fig. 3. The kinetics were of pseudo-first order (and treated accordingly) as the methanol was in large excess (this will be the case of the oxygenates considered in this study). The methanol concentration was varied from 1×10^{-2} to 4×10^{-2} mol L^{-1}. At 298 K, the measured rate constant is reported to be $(4.8 \pm 0.5) \times 10^5$ M^{-1} s^{-1}.

The previously reported rate constants for reaction R4 are in the range from 1.8 to 16×10^5 M^{-1} s^{-1}, with the latest determination by Herrmann and coworkers[20] being $(5.1 \pm 0.3) \times 10^5$ M^{-1} s^{-1}.

It appears that our measurement is in excellent agreement with the latter study where the experimental conditions were quite similar to our own conditions. This concerns especially the pH conditions which differ significantly from those used by Dogliotti and Hayon,[18] Pikaev *et al.*,[17] Neta and Huie,[21] Ito *et al.*[14] and Shastri and Huie.[16] All these studies were performed under very acidic conditions (*i.e.*, with a pH < 0) resulting apparently in most cases in slower reactions rates, by *ca.* 50% for the studies by Neta and Huie,[21] Ito *et al.*[14] and Shastri and Huie.[16]

However, the discrepancy between our studies and those by Dogliotti and Hayon and Pikaev *et al.* remains unclear. In fact, the rate coefficient reported in these studies should have been comparable to the first three quote at pH < 0 which are lower than those obtained under milder conditions (as those used here and by Herrmann and coworkers).

Table 1 Comparison of the room temperature rate coefficients for the reaction of the NO_3 radical with methanol obtained in this work with literature values

Author, year	Precursor	pH	T/K	Method	$10^5 \times k$/L mol^{-1} s^{-1}	Literature
Herrmann and Exner, 1994	$S_2O_8^{2-}/K_2Ce(NO_3)_6$	4.0	298	FP	5.1	13
Ito and Akiho, 1988	$K_2Ce(NO_3)_6$	<0	RT	FP	3.1	14
Neta and Huie, 1986	HNO_3	<0	295	PR	2.1	15
Shastri and Huie, 1990	HNO_3	<0	295	PR	1.8	16
Pikaev and Sibirskaya, 1974	HNO_3	<0	RT	PR	16.0	17
Dogliotti and Hayon, 1967	$K_2Ce(NO_3)_6$	7.0	RT	FP	10.0	18
This work	$S_2O_8^{2-}$	1.0	298	FP	4.8 ± 0.5	

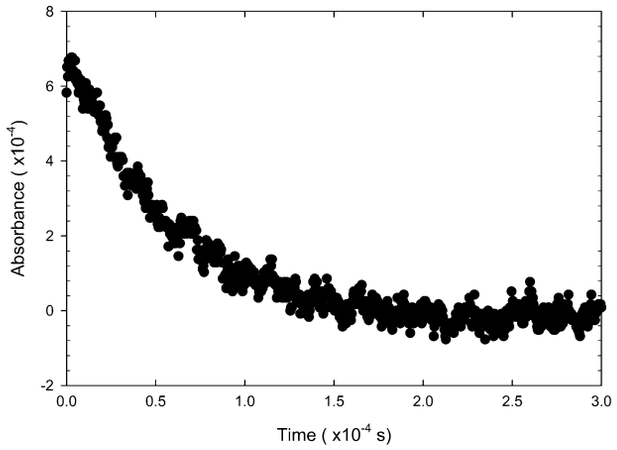

Fig. 2 Typical NO_3 temporal profile of the reaction $NO_3 + MeOH$ in 1M $HClO_4$ at 25 °C, $[NO_3^-] = 1M$, $[S_2O_8^{2-}] = 1M$ and $[MeOH] = 1.10^{-3}M$.

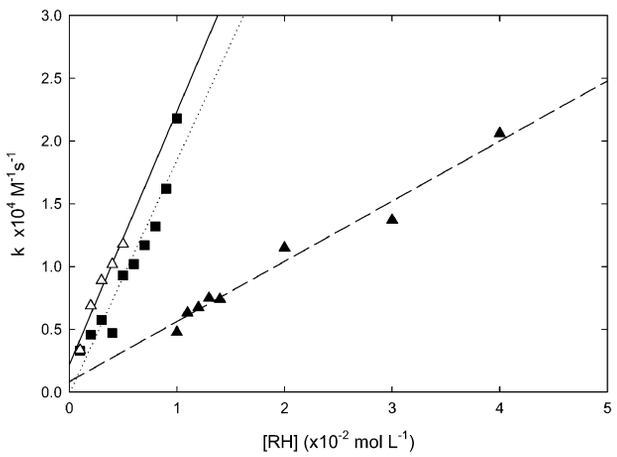

Fig. 3 Plots of the observed pseudo-first-order rate constants of NO_3 radicals for ▲ methanol, ■ ethanol and □ acetaldehyde in 1M HClO4 at 25 °C, $[NO_3^-] = 1M$ and $[S_2O_8^{2-}] = 1M$. The ordinates illustrate the kinetics of the reaction between the nitrate radical and its precursors or impurities.

However, just by considering the excellent agreement with the study by Herrmann and coworkers, we feel confident that the rate coefficient determined here is representative of the reaction between the nitrate radical and methanol under near-neutral conditions. This agreement, taken as a first step, can be a validation of our new technique.

NO_3 + ethanol

Many room temperature studies of the NO_3 + ethanol reaction kinetics are reported (see Table 2).

$$NO_3 + CH_3CH_2OH \rightarrow HNO_3 + CH_3CH_2OH \quad (R5)$$

A typical second order plot for this reaction is shown in Fig. 3. The rate coefficient determined in this study is $(1.9 \pm 0.3) \times 10^6$ M^{-1} s^{-1} at 298 K.

Previously reported rate coefficients are ranging from 1.1 to 3.9×10^6 M^{-1} s^{-1} (see Table 2). Therefore, our determination lies in the middle of the reported range. However again, we can notice an excellent agreement with the data reported by Herrmann and coworkers,[20] who measured a rate constant of $(2.4 \pm 0.5) \times 10^6$ M^{-1} s^{-1} under conditions directly comparable to the ones used here.

Again, all lower values presented in Table 2 were obtained in very acidic conditions (again with pH lower than 0) while the larger ones were measured at higher pH. The difference is again in the order of *ca.* 50%.

It may be speculated that both alcohols, under very acidic conditions, might exist in their protonated form. However, taking into consideration the pK_a of both alcohols, one can easily show that this fraction is very small. Therefore, this speculation has to be rejected as an explanation for the difference between all experiments, which differ by the reaction sequence used to produce the radicals. The main difference between these two approaches (*i.e.*, pulse radiolysis and laser photolysis) lies in the pH range applied. In fact, H-abstraction by NO_3 produces HNO_3 which is undissociated in 6 M HNO_3 (conditions employed in pulse radiolysis experiments) but fully dissociated under the conditions used in the present study. This additional dissociation process may provide additional energy to the system and therefore change the overall process. However, this is still speculative. Accordingly, this difference remains unresolved.

We can here only underline again that the results obtained in this work and by Herrmann *et al* compare quite favourably, which validates our experimental technique.

NO_3 + acetaldehyde

Less room temperature studies of the NO_3 + acetaldehyde reaction kinetics are reported in the literature (see Table 3).

$$NO_3 + CH_3CH(OH)_2 \rightarrow HNO_3 + CH_3C(OH)_2 \quad (R6)$$

For this aldehyde, or more exactly, for its gem-diol, we measured a second-order rate coefficient of $(2.0 \pm 0.3) \times 10^6$ M^{-1} s^{-1}, as listed in Table 3 while Herrmann *et al.*[20] measured $(1.9 \pm 0.6) \times 10^6$ M^{-1} s^{-1}. Again, both studies are in excellent agreement.

On the other hand, Ito *et al.*[22] measured a much higher rate coefficient (up to 6.2×10^6 M^{-1} s^{-1}), which cannot be directly reconciled with these two measurements. However, Ito *et al.*[22] performed their study at much higher ionic strength. Such a difference may partly explain the difference between Herrmann *et al.*,[20] our study and Ito *et al.*, as discussed by Herrmann and coworkers.

Finally, with the very good agreement with Herrmann and co-workers[20] (the single study directly comparable to our experimental conditions), we can argue that the experimental

Table 2 Comparison of the room temperature rate coefficients for the reaction of the NO_3 radical with ethanol obtained in this work with literature values

Author, year	Precursor	pH	T/K	Method	$10^6 \times k$/L mol^{-1} s^{-1}	Literature
Herrmann and Exner, 1994	$S_2O_8^{2-}/K_2Ce(NO_3)_6$	4.0	298	FP	2.4	13
Ito and Akiho, 1988	$K_2Ce(NO_3)_6$	<0	RT	FP	1.2	14
Neta and Huie, 1986	HNO_3	<0	295	PR	1.4	15
Shastri and Huie, 1990	HNO_3	<0	295	PR	1.1	16
Pikaev and Sibirskaya, 1974	HNO_3	<0	RT	PR	2.2	17
Dogliotti and Hayon, 1967	$K_2Ce(NO_3)_6$	7.0	RT	FP	3.9	18
Alfassi and Padmaja, 1993	$K_2Ce(NO_3)_6$	<0	296	FP	1.8	19
This work	$S_2O_8^{2-}$	1.0	298	FP	1.5 ± 0.3	

Table 3 Comparison of the room temperature rate coefficients for the reaction of the NO_3 radical with acetaldehyde obtained in this work with literature values

Author, year	Precursor	pH	T/K	Method	$10^6 \times k$/L mol^{-1} s^{-1}	Literature
Herrmann and Zellner, 1998	$S_2O_8^{2-}/K_2Ce(NO_3)_{66}$	4.0	297	FP	1.9	[2]
This work	$S_2O_8^{2-}$	1.0	298	FP	2.0 ± 0.3	

approach based on Teflon AF has successfully been validated and should, therefore, be applied to other studies.

Determination of new rate constants

In the atmosphere, the degradation of the dimethylmalonate, dimethylsuccinate, dimethylcarbonate, diethylcarbonate, *tert*-butyl ether and propionic acid will most likely be governed by the attack of OH and NO_3 radicals [*i.e.*, reactions (R7)–(R12)].

$$NO_3 + CH_3OC(O)CH_2C(O)OCH_3 \rightarrow H^+ + NO_3^- + CH_3OC(O)CH_2C(O)OCH_2 \quad (R7)$$

$$NO_3 + CH_3OC(O)CH_2CH_2C(O)OCH_3 \rightarrow H^+ + NO_3^- + CH_3OC(O)CH_2CHC(O)OCH_3 \quad (R8)$$

$$NO_3 + CH_3OC(O)OCH_3 \rightarrow H^+ + NO_3^- + CH_3OC(O)OCH_2 \quad (R9)$$

$$NO_3 + CH_3CH_2OC(O)OCH_2CH_3 \rightarrow H^+ + NO_3^- + CH_3CH_2OC(O)OCHCH_3 \quad (R10)$$

$$NO_3 + (CH_3)_3COCH_3 \rightarrow H^+ + NO_3^- + (CH_3)_3COCH_2 \quad (R11)$$

$$NO_3 + CH_3CH_2COOH \rightarrow H^+ + NO_3^- + CH_3CHCOOH \quad (R12)$$

The experimental approach described above was used to measure the bimolecular rate coefficients for the reactions of the NO_3 radical with dimethylmalonate (R7), dimethylsuccinate (R8), dimethylcarbonate (R9), diethylcarbonate (R10), *tert*-butyl methyl ether (R11) and propionic acid (R12). The pK_a of the latter acid is 4.87, therefore under our experimental conditions it can safely be assumed that this acid is undissociated.

Typical second order plots for these reactions are shown in Fig. 4 and all rate coefficients are summarised in Table 4.

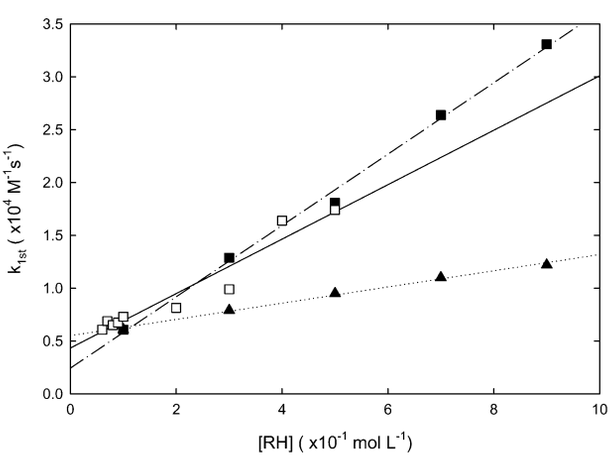

Fig. 4 Plots of the observed pseudo-first-order decay rates of NO_3 radicals for: ▲ propionic acid in 1M HClO4 at 25 °C, $[NO_3^-] = 1$M and $[S_2O_8^{2-}] = 1$M.; ■ dimethylsuccinate in 1M HNO_3 at 25 °C, $[[Ce^{IV}(NO_3)_6]^{2-}]$; □ dimethylmalonate in 1M HclO4 at 25 °C, $[NO_3^-] = 1$M and $[S_2O_8^{2-}] = 1$M. The ordinates illustrate the kinetics of the reaction between the nitrate radical and its precursors or impurities.

To our best knowledge, there are no other kinetic data for reactions (R7)–(R12) available in the literature with which to compare our results.

Discussion

Table 5 compares the reactivity of the different VOCs toward the nitrate and hydroxyl radicals. It obvious that the latter is reacting much more efficiently with all compounds. In fact, the ratio between both rate constants is ranging from 10^3 to 1.6×10^4. However, this limited set of data does not exhibit any specific trend.

A major assumption in the reactions studied above is that the NO_3 attack on the oxygenates proceeds *via* an H-abstraction mechanism. If the NO_3 attack proceeds *via* an H-abstraction, then the observed rate coefficients should be correlated with the type of bond and bond strength of the "leaving" hydrogen atom. The "leaving" hydrogen atom is probably the one having the weakest C–H bond strength (it was assumed that no H-abstraction occurs at the O–H group for alcohols). Bond dissociation energies (BDE) of the weakest C–H for all oxygenates are listed in Table 6. Other parameters listed in Table 6 are: (i) the number of equivalent hydrogen atom n_H (*i.e.*, those having the weakest bond strength); and (ii) the logarithm of the rate constant per H atom k_H, which is derived by:

$$k_H = k_{obs}/n_H \quad (1)$$

Many of the bond dissociation energies have not been experimentally measured and were, therefore, estimated using

Table 4 Summary of the rate coefficients for the reactions of the NO_3 radical with six oxygenates obtained in this work

Compounds	k/L mol^{-1} s^{-1}	NO_3 precursor
Diethylcarbonate	$(8.40 \pm 1.25) \times 10^4$	$S_2O_8^{2-}$
Dimethylcarbonate	$(1.5 \pm 0.4) \times 10^4$	$S_2O_8^{2-}$
Dimethylmalonate	$(2.6 \pm 0.7) \times 10^4$	$S_2O_8^{2-}$
Propionic acid	$(7.7 \pm 0.2) \times 10^4$	$S_2O_8^{2-}$
tert-Butyl-methyl ether	$(3.9 \pm 1.3) \times 10^5$	$K_2Ce(NO_3)_6$
Dimethylsuccinate	$(3.4 \pm 0.2) \times 10^4$	$K_2Ce(NO_3)_6$

Table 5 Comparison of the reactivity of the oxygenated compounds toward the nitrate and hydroxyl radicals. The data are from this work or ref. 5 and references cited therein

Reactant	k_{OH}/ L mol^{-1} s^{-1}	k_{NO3}/ L mol^{-1} s^{-1}	k_{OH}/ k_{NO3}
Methanol	$(1.3 \pm 0.4) \times 10^9$	$(4.8 \pm 0.5) \times 10^5$	2.7×10^3
Ethanol	$(1.9 \pm 0.5) \times 10^9$	$(1.9 \pm 0.3) \times 10^6$	$1.0 \times$ [3]
Dimethylmalonate	$(2.7 \pm 0.9) \times 10^8$	$(2.6 \pm 0.7) \times 10^4$	1.0×10^4
Dimethylsuccinate	$(5.3 \pm 2.9) \times 10^8$	$(3.4 \pm 0.2) \times 10^4$	1.6×10^4
Dimethylcarbonate	$(5.1 \pm 2.7) \times 10^8$	$(1.5 \pm 0.4) \times 10^4$	3.4×10^3
Diethylcarbonate	$(7.9 \pm 3.2) \times 10^8$	$(8.4 \pm 1.25) \times 10^4$	9.4×10^3
Acetaldehyde	3.6×10^{91}	$(2.0 \pm 0.3) \times 10^6$	1.8×10^3
tert-Butyl-methyl ether	1.6×10^{92}	$(3.9 \pm 1.3) \times 10^5$	4.3×10^3
Propionic acid	3.8×10^{83}	$(7.7 \pm 0.2) \times 10^4$	4.9×10^3

Table 6 Number of equivalent weak C–H bond (n_H) with the bond dissociation energy (BDE) and the rate constants k

Compounds	Equival H-atoms	BDE/ kJ mol^{-1}	k/L mol^{-1} s^{-1}
Methanol	3	393	$4.8 \pm 0.5 \times 10^5$
Ethanol	2	385	$1.5 \pm 0.3 \times 10^6$
Acetaldehyde	3	396	$2.0 \pm 0.3 \times 10^6$
Diethylcarbonate	2	424	$8.40 \pm 1.25 \times 10^4$
Dimethylcarbonate	3	432	$1.5 \pm 0.4 \times 10^4$
Dimethylmalonate	2	444	$2.6 \pm 0.7 \times 10^4$
Propionic acid	2	415	$7.7 \pm 0.2 \times 10^4$
tert-Butyl-methyl ether	3	397	$3.9 \pm 1.3 \times 10^5$
Dimethylsuccinate	4	424	$3.4 \pm 0.2 \times 10^4$

semi-empirical group contribution methods.[23,24] This method is independent of the one derived by S. Benson, as the latter does not allow the estimation of bond dissociation energies for complex oxygenated molecules. It should be underlined that these bond energies are, without doubt, carrying some uncertainties. However in the absence of experimental data, this estimation procedure is a straightforward solution that should still illustrate some trends in the rate constants.

It may be assumed that the observed differences of the reactivity of the NO_3 radical toward the organic species considered are due to changes in the activation energies which are expected to be linked to the bond dissociation energy of the bond being ruptured.[25] If this is the case, there should be a linear dependence of the logarithm of k_H on the bond strength. A plot of log(k_H) *versus* BDE is shown in Fig. 6. There is indeed a (weak) correlation between the logarithm of k_H and the bond strength, *i.e.* a decrease of the rate coefficient is observed with increasing BDE. As a result, the reaction of the NO_3 radical with oxygenates proceeds *via* an H-atom abstraction mechanism.

In summary, we reported in this study on the reactivity of the nitrate radical NO_3 toward several oxygenated compounds. For some of them, we measured the rate coefficient for the first time. Apparently, the reaction proceeds *via* an H-abstraction mechanism as already stated in previous studies. The existing data do not support any reliable estimation method, which warrants future work in order to improve knowledge that is required building reliable structure–activity relationships.

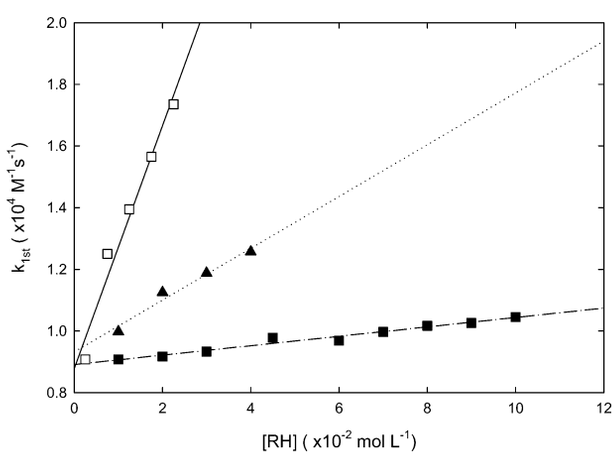

Fig. 5 Plots of the observed pseudo-first-order decay rates of NO_3 radicals for: ▲ diethylcarbonate; ■ dimethylcarbonate in 1M HclO4 at 25 °C, [NO_3^-] = 1M and [$S_2O_8^{2-}$] = 1M; □ *tert*-butyl-methyl ether. in 1M HNO_3 at 25 °C, [[$Ce^{IV}(NO_3)_6$]$^{2-}$] = 5.10^{-4} M. The ordinates illustrate the kinetics of the reaction between the nitrate radical and its precursors or impurities.

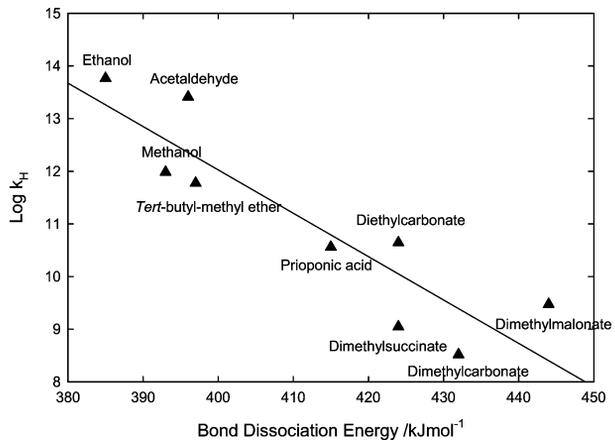

Fig. 6 Presentation of the logarithm of the rate constants per H atom abstractable *vs.* bond dissociation energies for NO_3 abstraction reactions in aqueous solution at room temperature.

Conclusions

This work addressed the oxidation of several oxygenated compounds by the nitrate radical using a newly developed experimental technique. The experimental approach described here takes advantage of the novel Teflon AF 2400 material. The physical nature of such tubing allows for the construction of photolysis reaction cells with very low volumes but potentially very long optical path lengths.

We have successfully applied such photolysis cell to the measurement of the rate coefficients for the liquid phase reaction of the nitrate radical with methanol, ethanol, acetaldehyde, *tert*-butyl methyl ether, propionic acid, dimethylmalonate, dimethylsuccinate, dimethyl carbonate and diethylcarbonate. The reported rate coefficients for the reactions of NO_3 with ethanol, methanol and acetaldehyde agree very well with the literature values. To date, there is no kinetic data reported for the OH radical reaction with dimethylmalonate, dimethylsuccinate, dimethylcarbonate, diethylcarbonate, *tert*-butyl methyl ether and propionic acid with which to compare our results.

Acknowledgements

Support of this work by the Programme National de Chimie Atmosphérique (PNCA) from the CNRS is gratefully acknowledged as well as the project PRIMEQUAL by the French Minister for Environment.

References

1 B. J. Finlayson-Pitts and J. N. Pitts, *Chemistry of the Upper and Lower Atmosphere: Theory, Experiments, and Applications*, Academic Press, San Diego, 2000.
2 H. Herrmann and R. Zellner, *N-Centered Radicals*, 1998, 291–343.
3 R. E. Huie, in *Laboratory Studies of Atmospheric Heterogeneous Chemistry; Current Problems in Atmospheric Chemistry, Advances in Physical Chemistry Series*, ed. J. R. Barker, World Scientific, Singapore, 1994, vol. 3, pp. 374–419.
4 T. Imamura, Y. Rudich, R. K. Talukdar, R. W. Fox and A. R. Ravishankara, *J. Phys. Chem. A*, 1997, **101**, 2316–2322.
5 C. George, D. Rousse, E. Perraudin and R. Strekowski, *Phys. Chem. Chem. Phys.*, 2003, **5**, 1562–1569.
6 M. Uusi-Penttila, R. J. Richards, P. Blowers, B. A. Torgerson and K. A. Berglund, *J. Chem. Eng. Data*, 1996, **41**, 235–238.
7 F. Cavalli, I. Barnes and K. H. Becker, *Int. J. Chem. Kinet.*, 2001, **33**, 431–439.

8 J. Wenger, E. Porter, E. Collins, J. Treacy and H. Sidebottom, *Chemosphere*, 1999, **38**, 1197–1204.
9 M. Bilde, T. E. Mögelberg, J. Sehested, O. J. Nielsen, T. J. Wallington, M. D. Hurley, S. M. Japar, M. Dill, V. L. Orkin, T. J. Buckley, R. E. Huie and M. J. Kurylo, *J. Phys. Chem. A*, 1997, **101**, 3514–3525.
10 M. A. Pacheco and C. L. Marshall, *Energy Fuels*, 1997, **11**, 2–29.
11 J. R. Odum, T. P. W. Jungkamp, R. J. Griffin, R. C. Flagan and J. H. Seinfeld, *Science (Washington, D. C.)*, 1997, **276**, 96–99.
12 J. H. Seinfeld, S. N. Pandis, *Atmospheric Chemistry and Physics: From Air Pollution to Climate Change*, Wiley, New York, 1998.
13 H. Herrmann, M. Exner and R. Zellner, *Geochim. Cosmochim. Acta*, 1994, **58**, 3239–3244.
14 O. Ito, S. Akiho and M. Iino, *Bull. Chem. Soc. Jpn.*, 1989, **62**, 1606–1611.
15 P. Neta and R. E. Huie, *J. Phys. Chem.*, 1986, **90**, 4644–4648.
16 L. V. Shastri and R. E. Huie, *Int. J. Chem. Kinet.*, 1990, **22**, 505–512.
17 A. K. Pikaev, G. K. Sibirskaya, E. M. Shirshov, P. Y. Glazunov and V. I. Spitsyn, *Dokl. Akad. Nauk SSSR*, 1974, **215**, 645–648.
18 L. Dogliotti and E. Hayon, *J. Phys. Chem.*, 1967, **71**, 3802–3808.
19 Z. B. Alfassi, S. Padmaja, P. Neta and R. E. Huie, *J. Phys. Chem.*, 1993, **97**, 3780–3782.
20 H. Herrmann, *Photochemische Bildung, Spektroskopie und Kinetik freier Radikale in wässeriges Lösung. Habilitationsschrift*, Universität GH Essen, 1997.
21 P. Neta and R. E. Huie, *J. Phys. Chem.*, 1986, **90**, 4644–4648.
22 O. Ito, S. Akiho and M. Iino, *J. Phys. Chem.*, 1989, **93**, 4079–4083.
23 J. Gasteiger, in *Physical Property Prediction in Organic Chemistry*, ed. C. Jochum, M. G. Hicks and J. Sunkel, Springer Verlag, Heidelberg, 1988, pp 119–138.
24 J. Gasteiger, 2000, PETRA: Parameter Estimation for the Treatment of Reactivity Applications, http://www2.chemie.uni-erlangen.de/software/petra/.
25 C. L. Clifton and R. E. Huie, *Int. J. Chem. Kinet.*, 1989, **21**, 677–687.

